# A Parameter Study of Stripline-Fed Vivaldi Notch-Antenna Arrays

Joon Shin and Daniel H. Schaubert, *Fellow, IEEE*

***Abstract*—A parameter study of Vivaldi notch-antenna arrays demonstrates that the wide-band performance of these antennas can be improved systematically. Stripline-fed Vivaldi antennas are comprised of: 1) a stripline-to-slotline transition; 2) a stripline stub and a slotline cavity; and 3) a tapered slot. The impedances of the slotline cavity and the tapered slot radiator combine at the transition to yield an equivalent series impedance on the feedline. The stripline stub can be represented by a series reactance. The resistance and reactance of the antenna impedance yield insights into the effects of various design parameters. In particular, it is found that the minimum operating frequency can be lowered primarily by increasing the antenna resistance through the change of design parameters. However, beyond a limit for each design parameter, the in-band performance begins to deteriorate. Plots of antenna impedance versus frequency for several parameter variations have been obtained by using a full wave method of moments analysis of infinite arrays. These plots provide a means for designers to systematically improve array performance with bandwidths in excess of 6 : 1 having been achieved.**

***Index Terms*—Notch antennas, phased array, ultrawide-band antenna.**

## I. Introduction

VIVALDI notch antennas can provide multioctave operation in phased arrays that scan over wide angles. Several examples have been built, e.g., [1]–[3]. When a successful design is achieved, its performance can sometimes be improved by varying the design slightly, but the relationships between antenna design parameters and array performance are not well understood. The performance of single antennas has been described and it has been found that single antennas work best when they are more than one wavelength long and when the height of the antenna aperture is greater than one-half wavelength [4], [5]. However, arrays of Vivaldi notch antennas perform best when the antennas are less than one wavelength long and when the element heights are much less than one-half wavelength [1]–[3], [6], [7]. This difference between the performance of isolated antennas and elements in arrays is due to mutual coupling effects, which can now be modeled accurately and efficiently by using numerical computations [7]–[9]. Thus, it is now possible to ascertain if a proposed design will work as desired. However, it is still difficult to determine what changes may be needed to improve the performance of a particular design.

This paper attempts to aid the antenna designer by identifying some of the relationships between the design of Vivaldi notch antennas and their performance in an array. The results of an extensive parameter study are presented in the form of active antenna impedances seen in a large array. The computational advantages of infinite periodic arrays are utilized, so these results are appropriate for the interior elements of large-phased arrays. A portion of a typical array is depicted in Fig. 1. The antennas studied here utilize a stripline feed coupled to bilateral slotlines (identical slots in both ground planes of the stripline). This is the type of design proposed in [10]. Other configurations have been studied by researchers: for example, asymmetric antennas with a single slotline and microstripline feed, antipodal fins fed by microstripline [5], and balanced antipodal versions [11]. These variations are not considered in this paper.

The parameter study reported here is carried out for ranges of parameters that include a "good" design, i.e., a design that works well over a 5 : 1 bandwidth. The parameter variations result in changes to the array's performance within its operating band and at the band edges. The results here are for arrays radiating in the broadside direction. It has been found that good performance at broadside is usually a positive indicator of good scan performance, although additional design considerations such as grid spacings, become important for wide scanning [6].

It has been found that the active input impedance of the antenna, resistance and reactance, at the point of the stripline-to-slotline transition is a useful indicator of the effects of parameter variations. Furthermore, since the upper operating frequency is limited by the onset of grating lobes, increased bandwidth is achieved by reducing the lowest frequency for which acceptable performance is obtained while maintaining in-band performance. The next section describes the parameters of the Vivaldi notch antenna and the method of analysis. Section III contains plots of active impedances for the antennas and discussions of the trends that have been observed.

## II. Method of Analysis

### A. Design Parameters of a Vivaldi Notch-Antenna Array

The design parameters of a Vivaldi notch-antenna array are defined in Figs. 1 and 2. They can be classified into three categories: substrate parameters (relative dielectric constant, $\epsilon_r$, and thickness, $t$), array grid parameters ($H$-plane spacing,

Manuscript received January 12, 1998. This work was supported in part by Army Research under Grant DAAL03-92-G-0295.

J. Shin was with the Department of Electrical and Computer Engineering, University of Massachusetts, Amherst, MA 01003 USA. He is now with the Department of Electrical Engineering, University of Mississippi, University, MS 38677 USA.

D. H. Schaubert is with the Department of Electrical and Computer Engineering, University of Massachusetts, Amherst, MA 01003 USA.

Publisher Item Identifier S 0018-926X(99)04834-6.

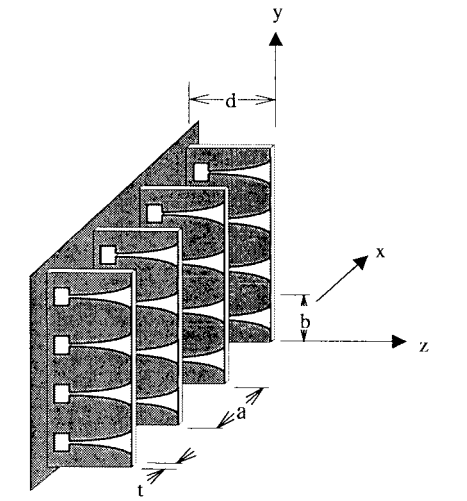


(a)

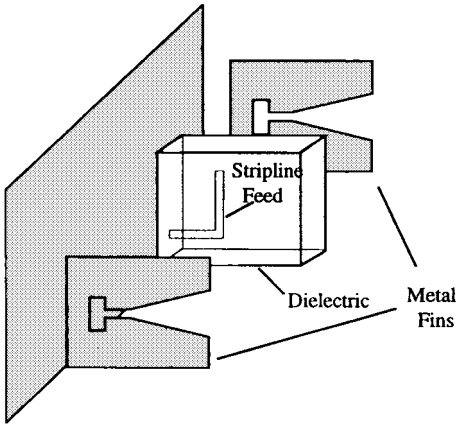


(b)

Fig. 1. (a) Portion of infinite stripline-fed Vivaldi notch-antenna array. (b) Exploded view of single element.

$a$, and $E$-plane spacing, $b$), and antenna element parameters, which can be subdivided into the stripline/slotline transition, the tapered slot, and the stripline stub and slotline cavity.

The stripline/slotline transition is specified by $W_{ST}$ (stripline width) and $W_{SL}$ (slotline width). The exponential taper profile is defined by the opening rate $R$ and two points $P_1(z_1, y_1)$ and $P_2(z_2, y_2)$

$$y = c_1 e^{Rz} + c_2 \tag{1}$$

where

$$c_1 = \frac{y_2 - y_1}{e^{Rz_2} - e^{Rz_1}}$$

$$c_2 = \frac{y_1 e^{Rz_2} - y_2 e^{Rz_1}}{e^{Rz_2} - e^{Rz_1}}.$$

The taper length $L$ is $z_2 - z_1$ and the aperture height $H$ is $2(y_2 - y_1) + W_{SL}$. In the limiting case where $R$ approaches zero, the exponential taper results in a so-called linearly tapered slot antenna (LTSA) for which the taper slope is constant and given by $s_o = (y_2 - y_1)/(z_2 - z_1)$. For the exponential taper defined by (1), the taper slope $s$ changes continuously from $s_1$ to $s_2$, where $s_1$ and $s_2$ are the taper slope at $z = z_1$ and at $z = z_2$, respectively, and $s_1 < s < s_2$ for $R > 0$. The taper flare angle is defined by $\alpha = \tan^{-1} s$.

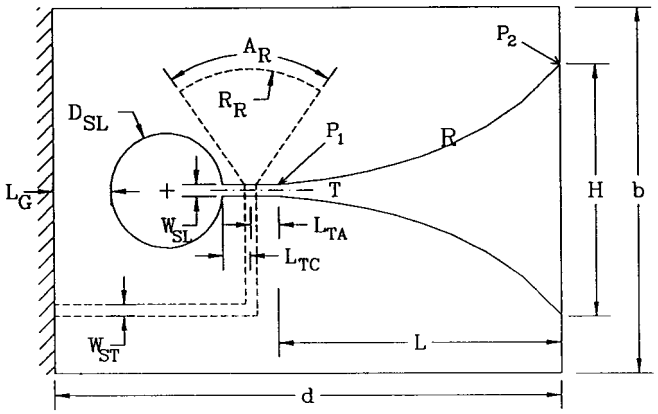


Fig. 2. Definition of parameters of Vivaldi notch-antenna element with circular cavity and radial stub.

The flare angles, however, are interrelated with and defined through other parameters, i.e., $H$, $L$, $R$, and $W_{SL}$.

The parameters related to the stripline stub and slotline cavity shown in Fig. 2 are as follows:

- $R_R$ radius of radial stripline stub;
- $A_R$ angle of radial stripline stub;
- $D_{ST}$ diameter of circular stripline stub [see inset of Fig. 4(b)];
- $D_{SL}$ diameter of circular slotline cavity;
- $L_G$ offset of slotline cavity from the ground plane;
- $L_{TC}$ distance from the transition to the slotline cavity;
- $L_{TA}$ distance from the transition to the taper.

In this study, $\epsilon_r$ is confined to the commonly used value of 2.2. Also, $L_{TC}$ and $L_{TA}$ are fixed to 0.25 cm. Experience indicates that $L_{TC}$ and $L_{TA}$ should be large enough to accommodate the stubs of the transition, but otherwise should be small. The shape and size of the stripline stub are not investigated explicitly in the parameter study. However, the effects of the stub can be extracted by using a simple equivalent circuit model as described below.

### *B. MoM Formulation and Equivalent Circuit Model*

The program used for computing the active input impedance of the arrays is based on the Green's function—moment method formulation [7]. It treats infinite phased arrays by analyzing the unit cell in detail. Triangular basis functions [12] have been added to improve the modeling capability for exponentially flared slots and impedance matrix interpolation [13] has been used to speed up the overall computations over a given frequency band.

In the equivalent circuit of Fig. 3, the total impedance $Z_{RP}$ at the reference plane $T$ on the stripline can be expressed as a series connection of the stripline stub reactance $jX_{STB}$ and the antenna impedance $Z_A$. The reference-plane impedance $Z_{RP}$ and the stub reactance $jX_{STB}$ are obtained by using the MoM program to analyze the full structure and a purely stripline structure without any slot, respectively. The equivalent circuit model has been validated by observing that the correct $Z_A$ is computed this way for stripline stubs of different shapes and sizes. It has been found that the stub reactance is independent of the array dimensions and scan angles, which is

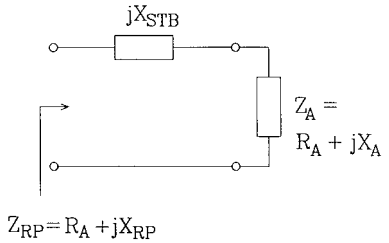


Fig. 3. Equivalent circuit for Vivaldi notch-antenna array element.

expected because the stripline is screened by the ground planes and does not introduce interelement interaction. By using this equivalent circuit, the role of the stripline stub in the wide-band performance of the arrays can be clearly understood in connection with the antenna impedance $Z_A$. Use of the equivalent circuit also reduces the number of parameters of the array since it eliminates the necessity of a parameter study involving different stub shapes and sizes. Although Knorr's equivalent circuit [14] has been used for single element antenna analysis [15] to further decompose $Z_A$ into a transformer followed by parallel-connected slotlines terminated by the cavity slot and the radiating tapered slot, it has been found not to work for quantitative analysis of wide-band phased arrays because the cavity slot and the tapered slot exhibit significant interaction with neighboring array elements. Therefore, the equivalent circuit of Fig. 3 treats the impedance of the antenna $Z_A$ as a single complex value that depends on frequency and scan angle as well as the parameters of the antenna.

## III. Results and Discussions

The parameter study is carried out in three sections: A—substrate thickness and stripline/slotline transition, B—slot parameters and backwall offset, and C—array grid spacings. All results are for $\epsilon_r = 2.2$ and $L_{TA} = L_{TC} = 0.25$ cm. Only one parameter (two for interrelated parameters) is varied at a time and all other parameters are fixed to the values specified below unless otherwise stated.

The proper selection of the stripline/slotline transition is crucial to the wide-band performance of the array. So, in Section III-A, various combinations of $W_{ST}$ and $W_{SL}$ have been studied for three different dielectric thicknesses. The array spacings are fixed to $a = 3.45$ and $b = 3.2$ cm. With these array dimensions, the upper frequency limit of interest is set to 5 GHz to ensure no grating lobes within $\pm 45°$ scan volume in both $E$- and $H$-planes, even though only the broadside results are presented here. All parameters except $R$ are set to the fixed values: $\epsilon_r = 2.2$, $a = 3.45$ cm, $b = 3.2$ cm, $L = 4.5$ cm, $H = 2.2$ cm, $D_{SL} = 1$ cm, $D_{ST} = 0.9$ cm, and $L_G = 0.5$ cm. The opening rate $R$ is varied from 0 to 0.7 to find the maximum impedance bandwidth over which standing-wave ratio (SWR) is less than two. Several "good" combinations have been found through this parameter study, i.e., combinations of $t$, $W_{ST}$, and $W_{SL}$ for which the bandwidth is larger than 4 : 1 at broadside scan.

In Section III-B, for one of the "good" choices of $t/W_{ST}/W_{SL} = 0.288/0.1/0.1$ cm, the effects on the active input impedance over 0.8–5.3 GHz are studied by varying each of the slot parameters ($L$, $H$, $R$, and $D_{SL}$) or the backwall offset ($L_G$) from its nominal value. The effects of the flare angles near the transition are studied through the variations of $L$, $H$, and $R$. The fixed or nominal values are: $\epsilon_r = 2.2$, $a = 3.45$ cm, $b = 3.2$ cm, $L = 4.5$ cm, $H = 2.2$ cm, $D_{SL} = 1$ cm, and $L_G = 0.5$ cm with a circular or radial stripline stub of proper size.

In Section III-C, the effects of varying the array grid spacings $a$ and $b$ are studied over 0.9–7 GHz with all other fixed or nominal parameters: $t = 0.288$ cm, $a = 2.5$ cm, $b = 1.7$ cm, $L = 4.5$ cm, $H = 1.7$ cm, $R = 0.3$, $D_{SL} = 1$ cm, $L_G = 0.5$ cm, $R_R = 0.8$ cm, and $A_R = 80°$.

TABLE I
Broadside Impedance Bandwidth: Substrate Thickness = 0.144 cm

| $W_{ST}$ \ $W_{SL}$ | 0.025 cm | 0.05 cm | 0.1 cm | 0.2 cm |
|---|---|---|---|---|
| 0.05 cm (81 Ω) | 1.87 5+ | 1.18 5+ | 1.12 5+ | 1.27 2.85 |
| 0.1 cm (56 Ω) | 1.84 5+ | 1.69 5+ | 1.48 3.04 | 1.53 2.51 |

TABLE II
Broadside Impedance Bandwidth: Substrate Thickness = 0.288 cm

| $W_{ST}$ \ $W_{SL}$ | 0.025 cm | 0.05 cm | 0.1 cm | 0.2 cm |
|---|---|---|---|---|
| 0.05 cm (109 Ω) | 1.13 2.88 | 1.08 3.35 | 1.12 5+ | 1.11 5+ |
| 0.1 cm (81 Ω) | 1.08 2.92 | 1.03 3.42 | 1.01 5+ | 1.06 5+ |
| 0.2 cm (56 Ω) | 2.27 5+ | 2.13 5+ | 1.02 2.82 | 0.95 2.94 |

TABLE III
Broadside Impedance Bandwidth: Substrate Thickness = 0.4 cm

| $W_{ST}$ \ $W_{SL}$ | 0.025 cm | 0.05 cm | 0.1 cm | 0.2 cm |
|---|---|---|---|---|
| 0.05 cm (123 Ω) | 1.7 2.68 | 1.16 2.97 | 1.19 3.37 | 1.18 5+ |
| 0.1 cm (94 Ω) | 1.09 2.83 | 1.11 3.03 | 1.08 5+ | 1.06 5+ |
| 0.2 cm (68 Ω) | 1.05 2.71 | 1.04 2.92 | 1.02 3.39 | 1.04 5+ |

### A. Substrate Thickness and Stripline/Slotline Transition

Tables I–III show broadside scan impedance bandwidths attainable by varying $R$ from 0 to 0.7 for various combinations of $W_{ST}$ and $W_{SL}$ and for dielectric thicknesses of $t = 0.144$, 0.288, and 0.4 cm, respectively. The shape of the antenna element is the same as that depicted in the inset of Fig. 7(b). The wide bars in the tables denote frequency bands over which the SWR is continuously less than 2.0. Several insights have been gained by studying these tables and many other cases that are not shown here. For example:

1) There appear to be many stripline-to-slotline combinations that result in bandwidths of larger than 4 : 1. Taking account of the unit-cell dimensions and restricting the parameters of Fig. 2 to reasonable values that fit within this space, the limit of the lower operating frequency ($f_L$) is about 1–1.2 GHz and that of the upper end ($f_U$) extends far above 5 GHz in some cases, but is set to 5 GHz to ensure no grating lobes in $\pm 45°$ scan volume. These "good" combinations have shown comparable wide-band performance at 45° scan in both $E$-plane and

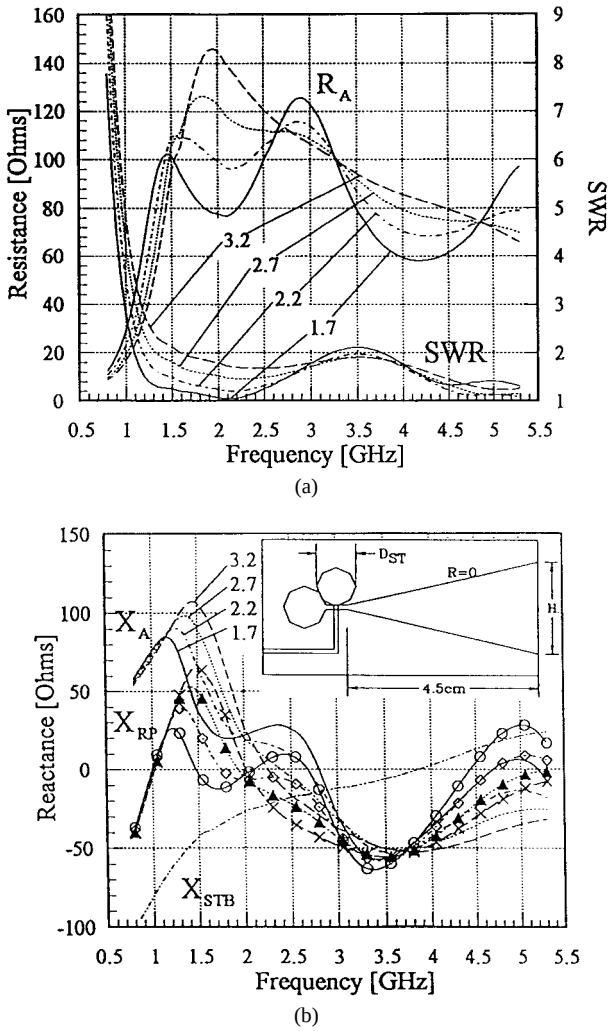


Fig. 4. Effects of aperture height on antenna impedance for $H = 1.7, 2.2, 2.7$, and $3.2$ cm with fixed antenna length, $L = 4.5$ cm. (a) Antenna resistance and SWR. (b) Antenna reactance (lines), reference-plane reactance (lines with points), and stub reactance.

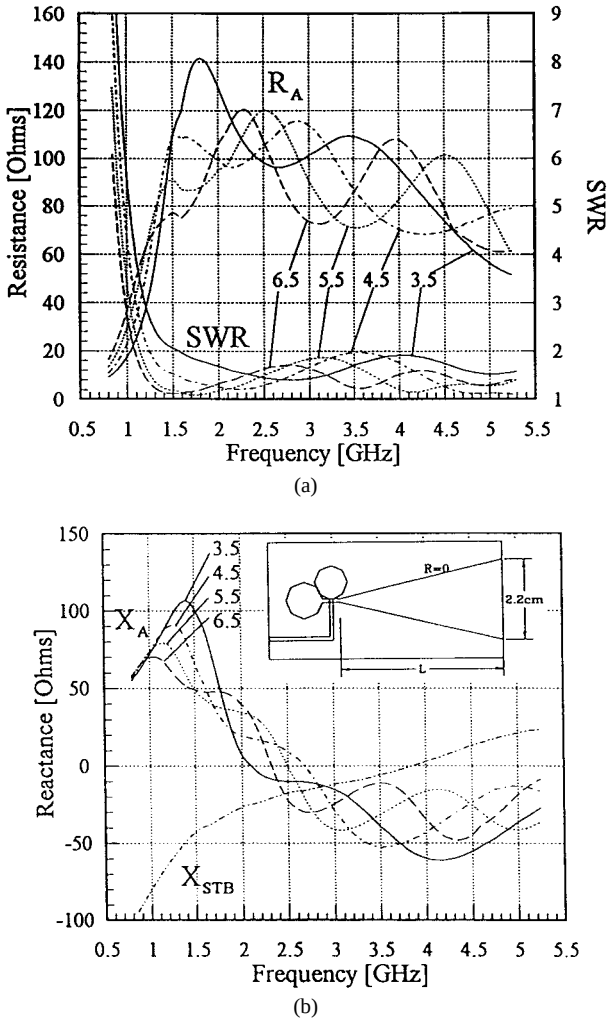


Fig. 5. Effects of taper length on antenna impedance for $L = 3.5, 4.5, 5.5$, and $6.5$ cm with fixed aperture height $H = 2.2$ cm. (a) Antenna resistance and SWR. (b) Antenna reactance and stub reactance.

$H$-plane, except the two cases of $t = 0.144$ cm with $W_{ST} = 0.05$ cm and $W_{SL} = 0.05$ and 0.1 cm for which $f_L$ is about 1.8 GHz for $H$-plane 45° scan.

2) The performance of the transition depends on the stripline stub and slotline cavity, the tapered slot, and the array spacing. For example, a different set of "good" combinations of $t/W_{ST}/W_{SL}$ have been obtained by using a uniform width stripline and a square-slot cavity [6].
3) Several cases involving "good" combinations of parameters have been checked for significantly reduced $a$ and/or $b$ and they still result in wide-band performance. Reducing $a$ and $b$ may be required to increase the upper frequency limit of a scanning array due to grating lobes and $H$-plane scan anomalies [6].

### B. Taper Parameters and Backwall Offset

The effects on the antenna impedances $Z_A = R_A + jX_A$ from changing parameters $H$, $L$, $R$, $L_G$ and $D_{SL}$, with all other parameters fixed to the values mentioned previously are presented in Figs. 4–9, together with the SWR performance and the stub reactances. In Fig. 4(b), the total reactances at the reference plane $jX_{RP} = j(X_{STB} + X_A)$ are also shown. The SWR at the reference plane $T$ is computed with respect to 81 Ω, the characteristic impedance of the stripline.

A detailed discussion of the effects of individual parameters is presented below. However, the general behavior of $Z_A$ can be summarized as follows for parameter values that are close to the nominal values listed above, which yield reasonably good performance.

1) The most important effect of each parameter change on the antenna impedance occurs around the lower end of the frequency band $f_L$. This effect is important for the operating bandwidth because the bandwidth, defined by the ratio $f_U/f_L$, changes significantly with a small change of $f_L$.
2) At the lower frequency end, the antenna resistance decreases rapidly toward zero, resulting in a sharp increase in SWR. This occurs because the slot cavity of finite size acts as a short circuit as the wavelength increases.
3) Above the lower end of the operating band $f_L$, the antenna resistance $R_A$ oscillates about the stripline characteristic impedance $Z_O$. In this study, where $t = 0.288$ cm, $W_{ST} = 0.1$ cm, and $\epsilon_r = 2.2$, $Z_O$ is 81Ω.

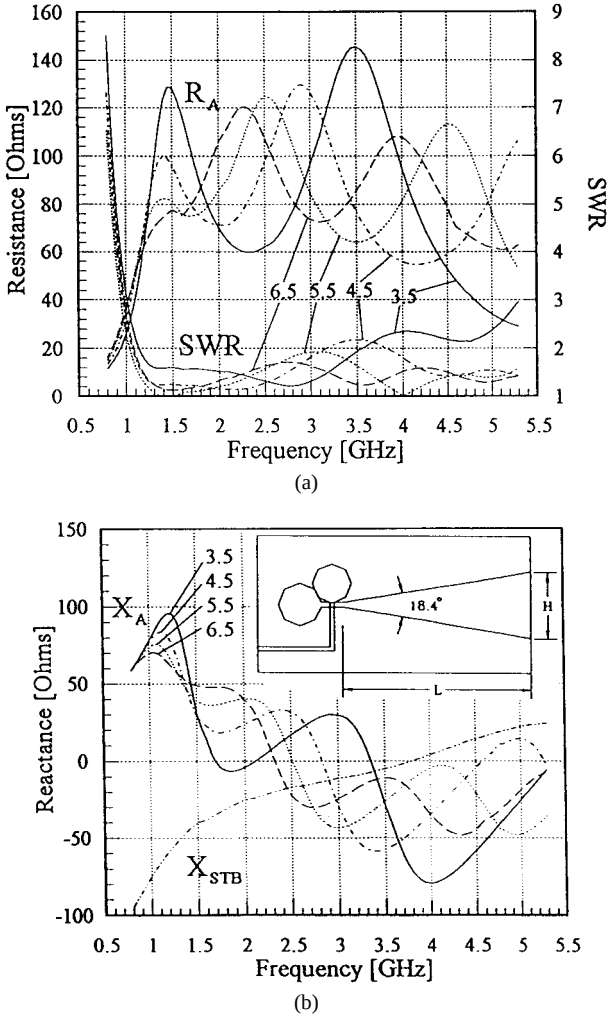


Fig. 6. Effects of taper length on antenna impedance for $L = 3.5, 4.5, 5.5,$ and $6.5$ cm with fixed flare angle. (a) Antenna resistance and SWR. (b) Antenna reactance and stub reactance.

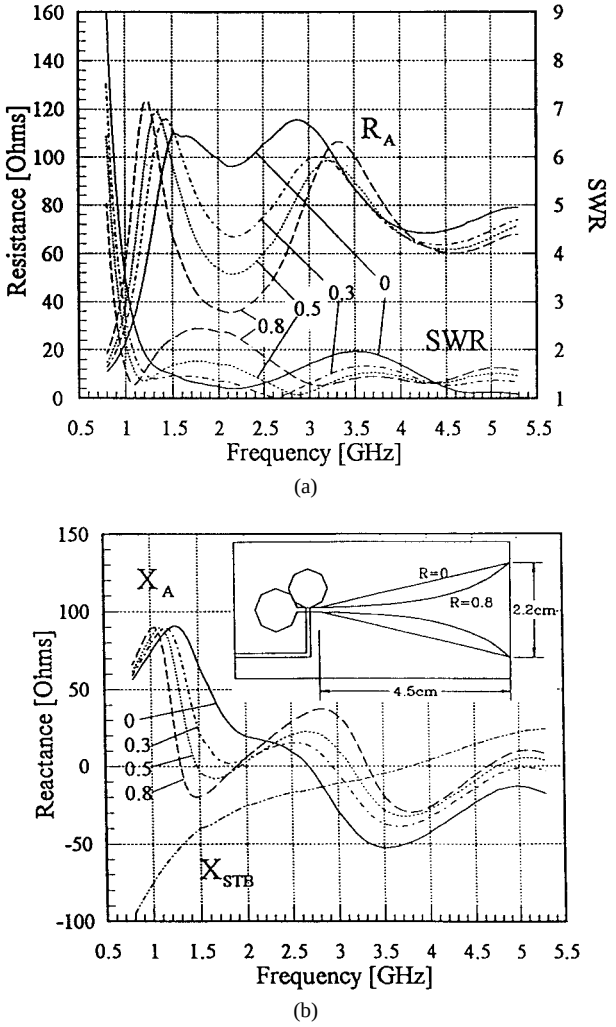


Fig. 7. Effects of opening rate on antenna impedance for $R = 0, 0.3, 0.5,$ and $0.8$. (a) Antenna resistance and SWR. (b) Antenna reactance and stub reactance.

4) The antenna reactance $jX_A = jX_{RP} - jX_{STB}$ oscillates near zero throughout much of the operating band. It has a large inductive peak around 1 GHz and then decreases toward zero in the lower frequencies. The capacitive reactance of the stripline stub at low frequencies partially cancels this inductive peak, improving overall performance at low frequencies.
5) It is observed that smaller flare angles near the transition, which correspond to larger $L$, smaller $H$, or larger $R$, result in improved SWR performance through the increase of the antenna resistance near $f_L$.

The stripline stub reactance of a radial stub or a circular stub varies from very large capacitive values in the lower frequencies, through a wide frequency range of near-zero reactance in the mid-band, to inductive values in the upper band. This behavior of the stub reactance results in favorable compensation of the antenna reactance, contributing to wideband performance. Uniform-width stripline stubs have a much greater rate of change of the reactance with frequency, which results in a maximum operating bandwidth of about $4:1$ over which the SWR is less than two. A radial or a circular stub can achieve about $6.5:1$ bandwidth for broadside scan. The maximum broadside impedance bandwidth is also dependent on the array spacings.

*1) Aperture Height—$H$:* Fig. 4 shows the effects of varying aperture height ($H = 1.7, 2.2, 2.7,$ and $3.2$ cm) for an LTSA with a fixed taper length of 4.5 cm and corresponding flare angles ($\alpha = 10.08°, 13.14°, 16.02°,$ and $19.01°$). For the results of Figs. 4–7, a circular stripline stub of $D_{ST} = 0.9$ cm has been used. The other parameters are fixed at the values in the beginning of Section III. A smaller aperture height results in improved lower end of the operating band $f_L$ through an increase of the antenna resistance $R_A$. It is the smaller flare angle that makes the antenna resistance increase with decreasing aperture height. The slightly increased SWR in the midband with decreasing $H$ is due to the increased capacitive antenna reactance $jX_A$. The amplitude of the periodic oscillations increases with decreasing aperture height, which causes a larger reflection from the aperture.

*2) Taper Length—$L$:* The effects of varying the taper length ($L = 3.5, 4.5, 5.5,$ and $6.5$ cm) for an LTSA with a fixed aperture height of 2.2 cm and corresponding flare angles ($\alpha = 16.7°, 13.14°, 10.81°,$ and $9.18°$) are shown in Fig. 5. Again, a smaller flare angle of the taper due to longer

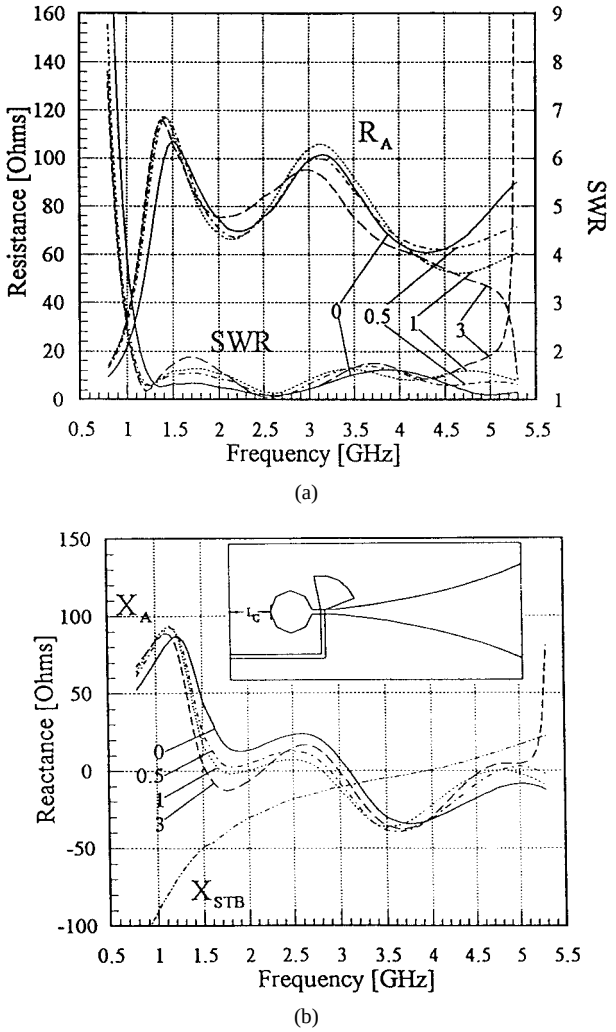


Fig. 8. Effects of backwall offset on antenna impedance for $L_G = 0,\ 0.5,\ 1,$ and 3 cm. (a) Antenna resistance and SWR. (b) Antenna reactance and stub reactance.

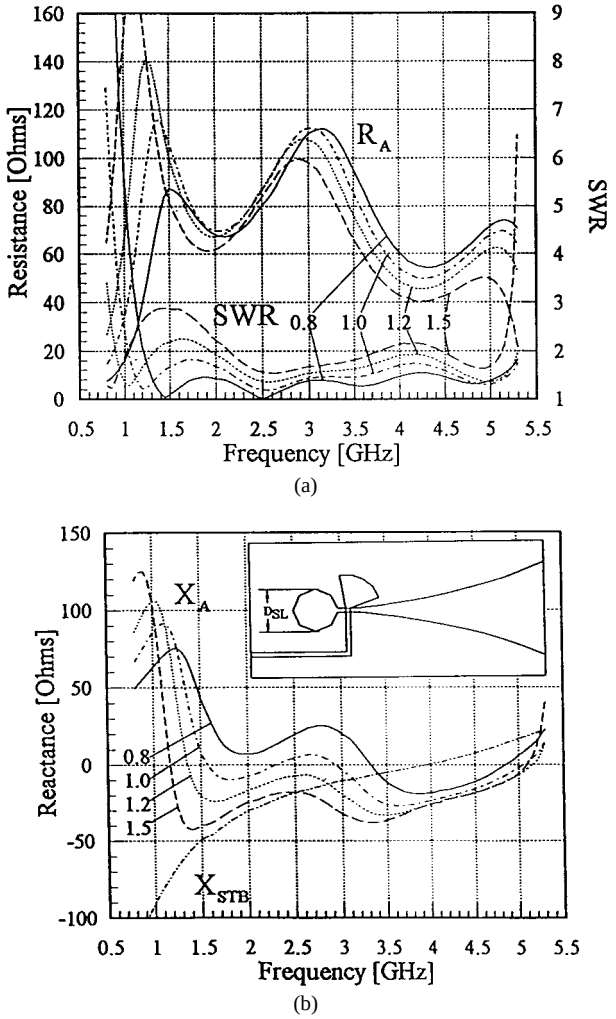


Fig. 9. Effects of size of slotline cavity on antenna impedance for $D_{SL} = 0.8,\ 1.0,\ 1.2,$ and 1.5 cm. (a) Antenna resistance and SWR. (b) Antenna reactance and stub reactance.

taper length results in increased antenna resistance near $f_L$, which, in turn, leads to improved $f_L$. The periods of the oscillations in $R_A$ and $X_A$, which are due to the reflections at the aperture plane, decrease as the taper length increases. The amplitude of the oscillations, however, do not change significantly by changing $L$ since the aperture height remains the same. Increasing $L$ also reduces the capacitive antenna reactance $jX_A$ in the mid-band to improve the mid-band SWR performance.

The effects of varying the taper length ($L = 3.5,\ 4.5,\ 5.5,$ and 6.5 cm) for an LTSA with a fixed flare angle $\alpha = 9.2°$, and corresponding aperture heights ($H = 1.20,\ 1.55,\ 1.88,$ and 2.20 cm) are shown in Fig. 6. This time, the effects of changing the taper length $L$ on the antenna resistance near $f_L$ are not so significant as in the previous cases of changing $H$ with a fixed $L$ and changing $L$ with a fixed $H$, both of which involve changing the flare angle $\alpha$. Thus, it seems that the small flare angles near the transition result in increased antenna resistances near the lower end of the band $f_L$. For shorter taper lengths, the expected longer periods of the antenna impedance oscillations are observed with increasing amplitudes due to the smaller aperture heights.

*3) Opening Rate—$R$:* The effects of varying the opening rate ($R = 0,\ 0.3,\ 0.5,$ and 0.8) with corresponding flare angles ($\alpha_1/\alpha_2 = 13.13°/13.13°,\ 6.29°/23.04°,\ 3.54°/30.41°,$ and $1.35°/40.81°$) are shown in Fig. 7. An improvement of $f_L$ through an increase of antenna resistance is observed for larger opening rates, which correspond to smaller flare angles near the transition. The larger opening rates also result in large changes of the antenna resistances in the frequency range from $f_L$ to about 3 GHz, which makes the first in-band hump of SWR increase. It is also observed that for larger opening rates, the SWR performance improves through the reduced capacitive antenna reactances above 3 GHz.

*4) Backwall Offset—$L_G$:* The effects of the backwall offset ($L_G = 0,\ 0.5,\ 1,$ and 3 cm) are shown in Fig. 8. For the results of Figs. 8 and 9, a radial stub of $R_R = 0.8$ cm and $A_R = 80°$ has been used. The increase of $L_G$ from 0 to 0.5 cm improves $f_L$ significantly through increases in both antenna resistance and inductive antenna reactance. Further increase of $L_G$ beyond 0.5 cm does not affect $f_L$ much, but raises the first in-band hump in SWR. There is a steep SWR increase at the upper frequency end for $L_G = 3$ cm. This has been found to be due to a broadside scan blindness at 5.315

GHz, which is explained and predicted by Schaubert [16]. The blindness is related to a surface wave on the equivalent corrugated surface that results from closing all of the slots in Fig. 1(a) with conductor.

*5) Size of Slotline Cavity—$D_{SL}$:* The effects of varying the size of the slotline cavity ($D_{SL} = 0.8$, 1, 1.2, and 1.5 cm) are shown in Fig. 9 with a fixed antenna depth of $d = 8$ cm and corresponding backwall offset $L_G = 2.2$, 2.0, 1.8, and 1.5 cm. From Fig. 9, it can be seen that a larger cavity improves $f_L$ greatly through increased antenna resistance and inductive antenna reactance, which is compensated by the large capacitive stub reactance. An excessively large cavity, however, introduces a large hump in the SWR near 1.5 GHz, which is due to the increased capacitive antenna reactance. At the upper frequency end, there is a steep increase of SWR. This has also been identified as the same kind of broadside scan blindness [16] occurring at 5.39 GHz for $D_{SL} = 1.5$ cm and slightly higher in frequency for smaller $D_{SL}$.

### C. Array Grid Spacings

The effects of varying the $H$-plane grid spacing ($a =$ 1.7, 2, 2.5, 3, and 3.45 cm) are shown in Fig. 10, with the $E$-plane grid spacing fixed to 1.7 cm. Reducing $a$ increases both the antenna resistances and reactances near $f_L$ and lowers $f_L$. However, it also increases the peak value of the antenna resistance and decreases the inductive reactance near 1.5 GHz, which results in a larger SWR hump. Since this first SWR hump usually gets larger for scan angles off broadside in the $H$-plane [6], the SWR at the first hump should be well below two in the broadside scan to achieve wide-scan performance. From 2 to 6 GHz, reducing $a$ does not change the antenna impedances significantly, although the amplitudes of the in-band SWR oscillations increase a little. The sharp increases in SWR at 6.27 GHz for $a = 3.45$ cm and at 6.97 GHz for $a = 3$ cm are again due to the $E$-plane scan blindnesses described in [16].

The effects of varying the $E$-plane grid spacing ($b =$ 1.7, 2, 2.5, and 3.2 cm) are shown in Fig. 11, with the $H$-plane grid spacing fixed to 2.5 cm. Increasing $b$ increases the amplitudes of the oscillations in both the antenna resistance and reactance over the frequency range. This is opposite to the effect of $H$-plane spacing, where increasing $a$ decreases the amplitude of the oscillations. The case of $b = 3.2$ cm can be compared with the case of $H = 1.7$ cm in Fig. 4 where all other parameters are similar except that $a = 3.45$ cm instead of 2.5 cm. Both cases have small aperture height ($H = 1.7$ cm) with large $E$-plane grid spacing ($b = 3.2$ cm) and have large amplitudes of impedance and SWR oscillations due to large reflections at the aperture. For smaller $E$-plane grid spacing (e.g., $b = 1.7$), it seems that the strong interactions between antenna elements in $E$-plane results in better impedance match at the aperture plane, even though the element height is small.

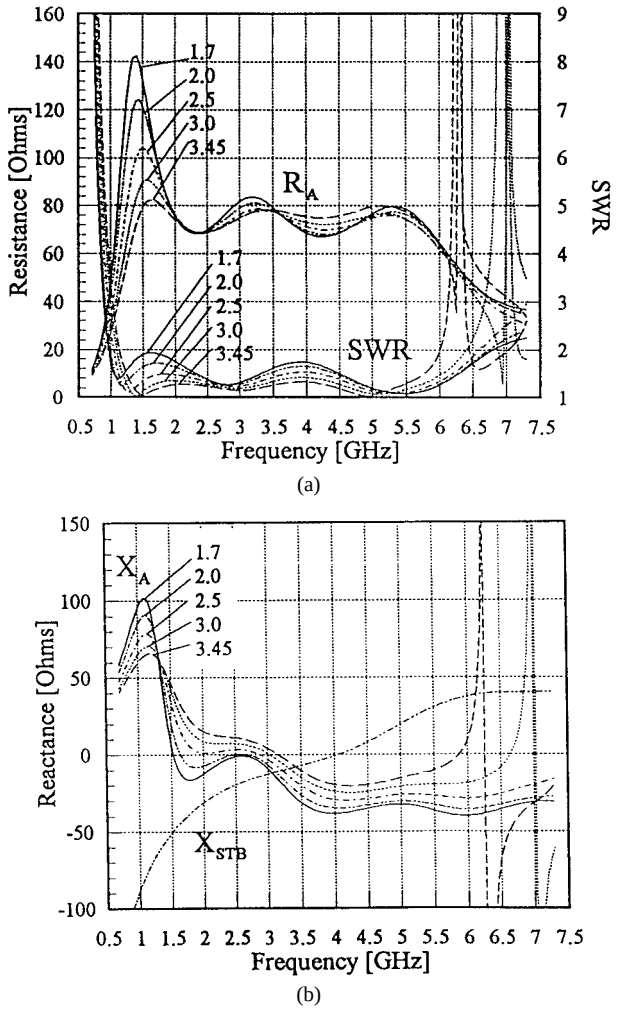


Fig. 10. Effects of $H$-plane grid spacing for $a = 1.7$, 2.0, 2.5, 3.0, and 3.45 cm. (a) Antenna resistance and SWR. (b) Antenna reactance and stub reactance.

## IV. Conclusions

An efficient, full wave method of moments analysis program has been used to study the effects of various design parameters on the performance of wide-band Vivaldi notch-antenna arrays. It has been found that the input impedance of the antenna, resistance and reactance, at the point of the stripline-to-slotline transition is a useful indicator of the effects of parameter variations. Furthermore, since the upper operating frequency is limited by the onset of grating lobes, increased bandwidth is achieved by reducing the lowest frequency for which acceptable performance is obtained while maintaining in-band performance. Many parameters can be used to achieve wider bandwidth by lowering the minimum operating frequency, but a limit is reached when in-band performance deteriorates. Contrary to observations for single antennas, array elements perform better when the antenna height is much less than one-half wavelength. Many antennas operate well at frequencies as low as 1 GHz. At this frequency, the aperture is only 0.06–0.07 wavelengths and the total array depth back-wall-to-aperture is less than 0.25 wavelength.

The open-circuit stripline stub does not radiate and can be adequately described by a series reactance. Typical stub configurations can be evaluated separately from the antenna array and their reactances used in the equivalent circuit. The reactance variation of the stub is opposite that of the antenna over much of the frequency band, which results in improved overall performance. It has been found that the reactance vari-

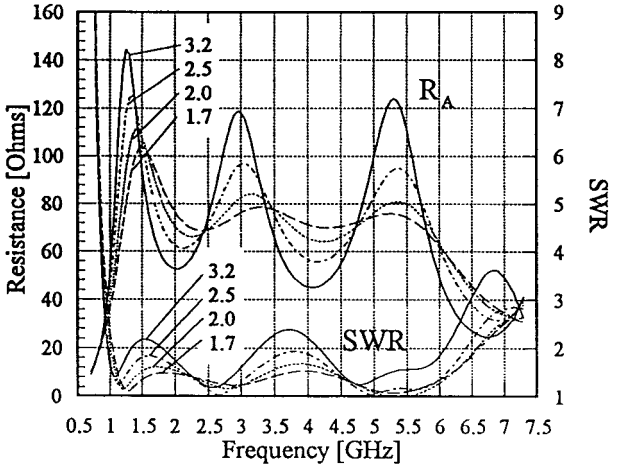


(a)

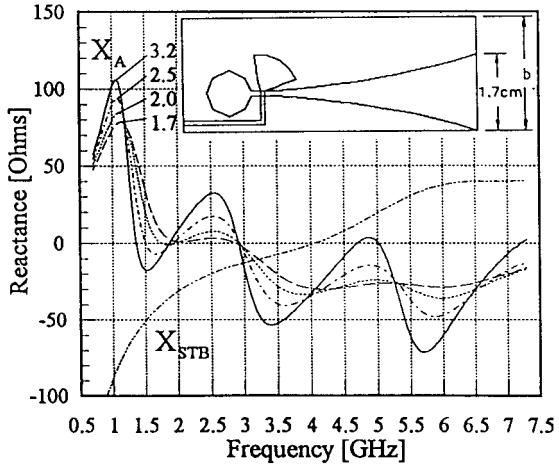


(b)

Fig. 11. Effects of $E$-plane grid spacing for $b = 1.7, 2.0, 2.5,$ and $3.2$ cm. (a) Antenna resistance and SWR. (b) Antenna reactance and stub reactance.

ation of radial and circular stubs is better suited for wide-band operation than is the reactance of constant linewidth stubs.

The antenna impedances are shown in the figures. By using the results in Figs. 4–11, a trial array of Vivaldi notch antennas has been systematically redesigned to yield operating bandwidths in excess of $6:1$. Many of the trends observed in Figs. 4–11 have been observed in other similar Vivaldi notch-array designs, but the available data do not provide enough cases to set limits on the extrapolation of the present work. Efficient numerical simulations that permit the designer to observe variations of $R_A$ and $X_A$ continue to be important for wide-band Vivaldi notch-array design. Future work will explore the scan performance of these wide-band arrays attempting to improve the performance of scanning arrays. Preliminary results have yielded $5:1$ bandwidth for scanning to 45° in both the $E$-plane and $H$-plane.

## REFERENCES

[1] J. Pozgay, "Wideband sub-array radiator for advanced avionics applications," in *Proc. Antenna Applicat. Symp.,* Allerton Park/Monticello, IL, Sept. 1992.

[2] S. Sanzgiri, "Observed phenomena in flared notch element arrays," presented at Panel discussion on wide-band Vivaldi notch antennas and arrays, presented at *IEEE Antennas and Propagation Symp.*, Newport Beach, CA, June 1995.

[3] M. J. Povinelli, "Experimental design and performance of endfire and conformal flared slot (notch) antennas and application to phased arrays: An overview of development," in *Proc. Antenna Application Symp.*, Allerton Park/Monticello, IL, Sept. 1988.

[4] K. S. Yngvesson, T. L. Korzeniowski, Y. S. Kim, E. L. Kollberg, and J. F. Johansson, "The tapered slot antenna—A new integrated element for millimeter-wave applications," *IEEE Trans. Microwave Theory Tech.*, vol. MTT-37, pp. 365–374, Feb. 1984.

[5] E. Gazit, "Improved design of the Vivaldi antenna," *Proc. Inst. Elect. Eng.*, vol. 135, pt. H, pp. 89–92, Apr. 1988.

[6] J. Shin and D. H. Schaubert, "Toward a better understanding of wideband Vivaldi notch antenna arrays," in *Proc. Antenna Application Symp.*, Allerton Park/Monticello, IL, Sept. 20–22, 1995.

[7] D. H. Schaubert, J. A. Aas, M. E. Cooley, and N. E. Buris, "Moment method analysis of infinite stripline-fed tapered slot antenna arrays with a ground plane," *IEEE Trans. Antennas Propagat.*, vol. 42, pp. 1161–1166, Aug. 1994.

[8] P. S. Simon, K. McInturff, R. W. Jobsky, and D. L. Johnson, "Full-wave analysis of an infinite planar array of linearly polarized stripline-fed notch elements," in *Dig. IEEE Antennas and Propagation Symp.*, London, ON, Canada, June 1991, pp. 334–337.

[9] J. Shin, "Improved method of moments computations applied to tapered slot antenna arrays," M.S. thesis, Elect. Comput. Eng., Univ. Massachusetts, Amherst, MA, Sept. 1994.

[10] L. R. Lewis, M. Fasset, and J. Hunt, "A broadband stripline array element," in *Dig. IEEE Antennas and Propagation Symp.*, Atlanta, GA, June 1974, pp. 335–337.

[11] J. D. S. Langley, P. S. Hall, and P. Newham, "Novel ultrawide-bandwidth Vivaldi antenna with low crosspolarization," *Electron. Lett.*, vol. 29, pp. 2004–2005, Nov. 1993.

[12] S. M. Rao, D. R. Wilton, and A.W. Glisson, "Electromagnetic scattering by surfaces of arbitrary shape," *IEEE Trans. Antennas Propagat.*, vol. AP-30, pp. 409–418, May 1982.

[13] E. H. Newman, "Generation of wide-band data from the method of moments by interpolating the impedance matrix," *IEEE Trans. Antennas Propagat.*, vol. 36, pp. 1820–1824, Dec. 1988.

[14] J. B. Knorr, "Slot-line transitions," *IEEE Trans. Microwave Theory Tech.*, vol. MTT-22, pp. 548–554, May 1974.

[15] D. H. Schaubert, "Endfire slotline antennas," *Journees Internationales de Nice sur les Antennes*, Nice, France, Nov. 1990, pp. 253–265.

[16] ———, "A class of E-plane scan blindnesses in single-polarized arrays of tapered slot antennas with a ground plane," *IEEE Trans. Antennas Propagat.*, vol. 44, pp. 954–959, July 1996.

**Joon Shin** was born in Korea on March 17, 1955. He received the B.S. and M.E. degrees (electrical engineering) from KyungPook National University, Korea, in 1981 and 1983, respectively, and the M.S. degree (electrical engineering) from the University of Massachusetts at Amherst in 1994. He is currently working toward the Ph.D. degree at the University of Mississippi

From 1982 to 1991, he was employed at the Electromagnetics Laboratory, Korea Research Institute of Standards and Science, working on the development of RF and microwave measurement standards and techniques. Since August 1996 he has been a Graduate Assistant in electrical engineering at the University of Mississippi. His current interest is in the use of the method of moments and the finite-difference time-domain analysis.

**Daniel H. Schaubert** (S'68–M'74–SM'79–F'89) has been with the University of Massachusetts at Amherst since 1982 and is currently a Professor of electrical and computer engineering. Prior to joining the faculty there, he was Lead Scientist for the analysis of electromagnetic problems at the National Center for Devices and Radiological Health, Rockville, MD, and he was a Research Engineer at the Harry Diamond Laboratories near Washington, DC. He coedited *Microstrip Antennas* (New York: IEEE Press, 1995).

Dr. Schaubert has been active in the IEEE Antennas and Propagation Society as President, Vice President, two terms on the Administrative Committee, Secretary-Treasurer, Newsletter Editor, Distinguished Lecturer Program Coordinator, and chapter offices in Washington, DC. He was also Associate Editor of IEEE TRANSACTIONS ON ANTENNAS AND PROPAGATION. He participated in the steering committees for the 1978, 1984, and 1996 annual symposiums and organizes the annual Antenna Applications Symposium.